Chemical Engineering Journal 162 (2010) 341–349

Contents lists available at ScienceDirect

Chemical Engineering Journal

journal homepage: www.elsevier.com/locate/cej

Selective oxidation of *p*-cymene catalyzed by VPO catalyst: Process performance and kinetics studies

Peter R. Makgwane[a,*], Nigel I. Harmse[a], Ernst E. Ferg[b], Ben Zeelie[a]

[a] *InnoVenton: NMMU Institute of Chemical Technology, Nelson Mandela Metropolitan University, P.O. Box 77000, Port Elizabeth, 6031, South Africa*
[b] *Department of Chemistry, Nelson Mandela Metropolitan University, P.O. Box 77000, Port Elizabeth, 6031, South Africa*

ARTICLE INFO

Article history:
Received 2 March 2010
Received in revised form 6 May 2010
Accepted 8 May 2010

Keywords:
Vanadium phosphate
Liquid phase oxidation
p-cymene
Tertiary cymene hydroperoxide
Kinetics

ABSTRACT

The catalyzed liquid phase oxidation process of *p*-cymene to tertiary cymene hydroperoxide (TCHP) by vanadium phosphorous oxide (VPO) catalysts was studied in a well-stirred batch reactor. It was found that the VPO compounds improve the *p*-cymene oxidation rates and selectivity towards TCHP. In particular, the process gave around 85% TCHP selectivity with conversion of about 30% achieved within 4 h when compared to long oxidation times (8–12 h) in non-catalyzed industrial-scale *p*-cymene oxidation process. Although catalysts material containing the vanadyl pyrophosphate phase ((VO)2P2O7) are more active and selective, there is no evidence that this phase is the solely required active phase for this type of oxidation reaction based on the results of the tested different VPO catalyst phases. The results indicated the active participation of the catalyst in the initiation of the oxidation process, thus, reducing the long induction period. In the presence of only initiator added (ROOH), the reaction initiation showed typical long induction period of about 5–6 h to form only about 1% conversion. The observed improved TCHP selectivity displayed by the VPO catalyst during normal oxidation reaction can be explained by the slow or insignificant influence of the catalyst on the decomposition rate of the formed TCHP to by-products at substrate conversions of 35% or less. A kinetic model was determined that fitted the experimental results to predict the performance of the *p*-cymene liquid phase oxidation rates and conversion.

1. Introduction

Selective oxidations of hydrocarbons are of major industrial importance in the production of intermediate oxygenated chemicals [1]. The improvement of their process efficiency and selectivity remains the prime important objective in many chemicals production processes [1,2]. The cymene–cresol process is one of such oxidation processes that facilitate the production of *m*- and *p*-cresols from the corresponding cymene hydroperoxides [2,3]. As is the case in the analogous cumene-phenol process, the cymene–cresol process also consists of three fundamental chemical reaction steps; (1) preparation of cymene by alkylation of toluene with propylene; (2) oxidation of the cymene to form cymene hydroperoxide (CHP); and (3) the acid cleavage of the CHP to cresol and acetone [4,5]

The cymene–cresol process has a low space-time yield that is 20–30% lower than the corresponding cumene-phenol oxidation process [2,3,6]. The conversions in the industrial-scale cymene–cresol oxidation process are restricted to 15–20% at 8–12 h reaction times as to preserve the selectivity towards tertiary cymene hydroperoxide (TCHP) which is in a range of 60–70% [2]. This is due to the formation of the by-product *p*-methylacetophenone (**11**) that increases rapidly at higher conversions from the thermal decomposition of the TCHP (**10**) as illustrated in Scheme 1. In addition to the formation of TCHP from the isopropyl group, the methyl group is also oxidized to primary cymene hydroperoxide (PCHP) (**4**) which react further to form by-products such as *p*-isopropyl benzaldehyde (**5**), *p*-isopropyl benzoic acid (**6**) and *p*-isopropyl benzyl alcohol (**7**). The ratio of methyl group to isopropyl group oxidation rate in *p*-cymene oxidation process has been reported to be 1:4 [2]. A further drawback of the PCHP formation during the oxidation process is that in the acid cleavage step, the PCHP can decompose to isopropyl phenol and formaldehyde. The formaldehyde, in turn, reacts with cresol to form cresol-formaldehyde resin that reduces the cresol yield and complicates the processing of the product work-up [3,6]. As a result, the PCHP is removed using aqueous solution of NaOH prior the acid cleavage step of the TCHP to *p*-cresol.

Various solutions to the shortcomings of the *p*-cymene oxidation process have been proposed. These include the continuous decomposition of the formed PCHP during the oxidation process together with the extraction of decomposition products [2,3]. This is the basis of current commercial operations in which

---

* Corresponding author. Tel.: +27 41 504 3640; fax: +27 41 504 3442.
E-mail address: peter.makgwane@gmail.com (P.R. Makgwane).

1385-8947/$ – see front matter © 2010 Elsevier B.V. All rights reserved.
doi:10.1016/j.cej.2010.05.016

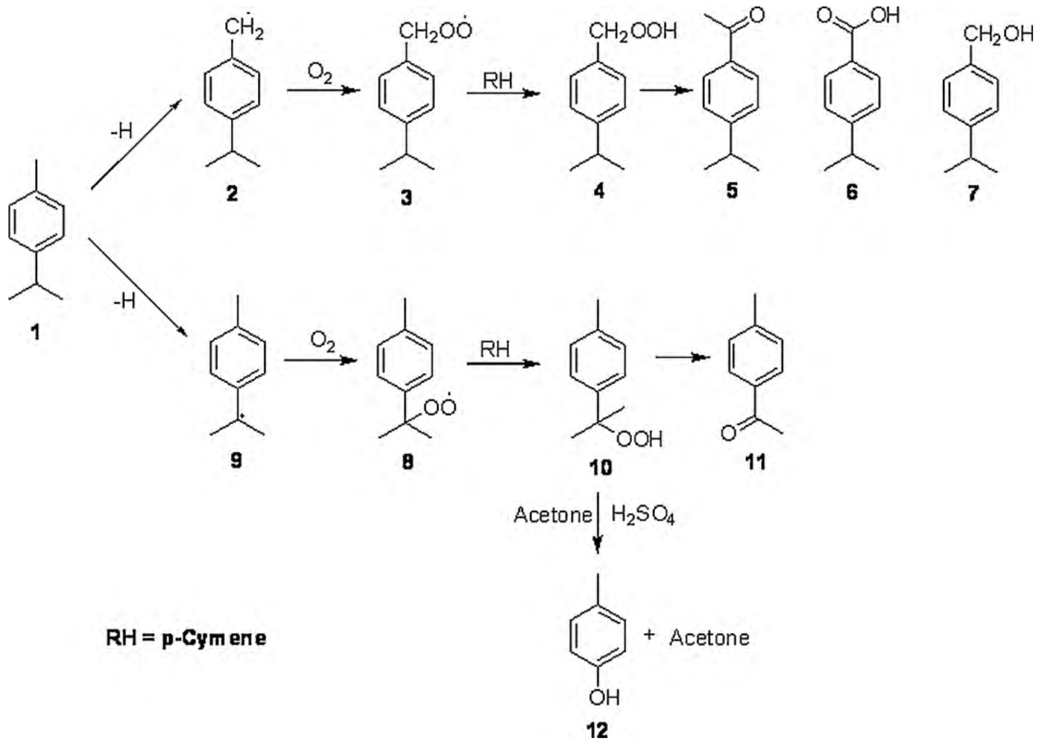

Scheme 1. Liquid phase *p*-cymene oxidation products [28].

the *p*-cymene is oxidized in a two-phase reaction system that comprises of an aqueous basic phase and organic phase [2]. In view of the process aspects inefficiencies discussed in the current industrial-scale non-catalyzed *p*-cymene oxidation process there is a need for a cleaner catalyzed process using heterogeneous catalysts to improve both the oxidation rates and product selectivity. The use of vanadium phosphorous oxide (VPO) catalysts for selective gas phase oxidation of C_2-C_5 hydrocarbons and others is well known [7–15]. While the VPO catalyst proved to possess interesting catalytic properties, very few studies have reported the application of VPO catalyst in liquid phase oxidations [16–23].

In this paper, we studied the catalytic performance of $(VO)_2P_2O_7$ catalyst prepared by three distinctive different preparation methods via $VOHPO_4{\cdot}0.5H_2O$ precursor in liquid phase oxidation process of *p*-cymene. The said oxidation was done in the absence of a solvent and aqueous phase with the view to minimize the waste generation and the formation of PCHP thereby increasing the overall process rates and the TCHP selectivity in a well-stirred batch reactor. In addition, the influences of different process parameters on the oxidation rates were investigated. By using the extensive studied kinetic model of cumene, it was possible to be able to evaluate the kinetic performance of the *p*-cymene oxidation process [4,5].

2. Experimental

2.1. Catalyst preparation methods

Three distinctive standard methods were used to prepare the VPO catalyst precursors phase, $VOHPO_4{\cdot}0.5H_2O$ [14]. In the first method, the precursor was prepared in an aqueous medium by dissolving V_2O_5 (6.0 g; 33 mmol) in aqueous HCl (35%, 79 mL) and refluxing for 2 h. The H_3PO_4 (85%; 8.9 g; 78 mmol) was added and the solution refluxed for further 2 h. The solution was subsequently evaporated to dryness and the resulting solid was refluxed in water (20 mL $H_2O\,g^{-1}$ solid) for 1 h. It was then filtered hot, washed with warm water, and dried in air (110 °C, 16 h). The precursor prepared by this method is denoted P1.In the second method, the precursor was prepared in an organic medium, by adding V_2O_5 (11.8 g; 66 mmol) to isobutanol (250 mL). H_3PO_4 (85%; 16.4 g; 39 mmol) was then introduced and the whole mixture was refluxed for 16 h. The light blue suspension was then separated from the organic solution by filtration and washed with isobutanol (200 mL) and ethanol (150 mL, 100%). The resulting solid was refluxed in water (9 mL g^{-1} solid), filtered hot, and dried in air (110 °C, 16 h). The precursor prepared by this method is denoted P2. The third method precursor was prepared via the dihydrate compound $VOPO_4{\cdot}2H_2O$. A mixture V_2O_5 (11.8 g; 66 mmol) and H_3PO_4 (85%; 115.5 g; 106 mmol) were refluxed in water (24 mL g^{-1} solid) for 8 h. The resulting $VOPO_4{\cdot}2H_2O$ was recovered by filtration and washed with a little water. Some of the $VOPO_4{\cdot}2H_2O$ (4.0 g; 20 mmol) was subsequently refluxed with isobutanol (80 mL) for 21 h, and the resulting solid was recovered by filtration and dried in air (110 °C, 16 h). The precursor prepared by this method is denoted P3. The precursors (P1, P2 and P3) were activated under N_2 flow in the tube furnace at 550 °C for 4 h. They are denoted C1, C2 and C3, respectively.

2.2. Catalyst characterization techniques

Ambient temperature powder X-ray diffraction (XRD) measurements were obtained using a Bruker D8 using Cu Kα radiation in standard Bragg–Brentano geometry using a Ni filter at the detector. The scan range of 2θ was 5–60° at 0.02 steps. The surface area of the catalysts samples were determined by BET nitrogen absorption using a Gemini Micromeritics surface area analyzer. Samples were first degassed at 170 °C for 2 h prior to analysis. Particle size analysis was done by laser diffraction of a dispersed aqueous suspension on a Malvern Mastersizer particle size analyzer equipped with a MS 17 automated sample dispersion unit.

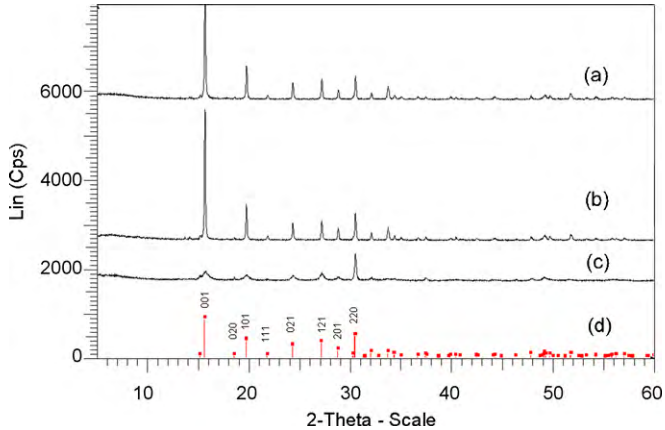

Fig. 1. XRD patterns of the $VOHPO_4·0.5H_2O$ precursors prepared by different methods. (a) P1 precursor; (b) P2 precursor; (c) P3 precursor; (d) XRD library reference PDF file JCP2 00-047-0953 [25].

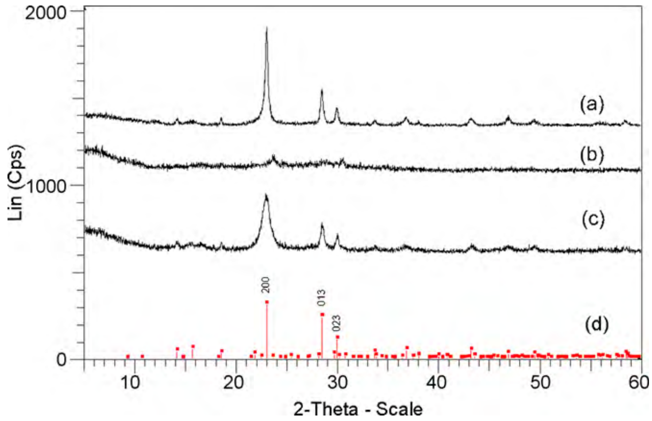

Fig. 2. XRD patterns of the calcined $(VO)_2P_2O_7$ catalyst from different precursors (a) C1 catalyst; (b) C2 catalyst; (c) C3 catalyst; (d) XRD library reference PDF file JCP2 00-0053-1051 [25].

2.3. Oxidation and catalyst testing procedure

Catalytic testing was performed at atmospheric pressure in a jacketed 500 mL glass batch reactor fitted with two baffles and impeller-type stirrer blade. To a reactor was added *p*-cymene (35 g, 261 mmol), oxidized cymene hydroperoxide (CHP) oil as initiator (2 g) to initiate the reaction (containing 58% content of TCHP) and the respective VPO catalysts (0.05–0.1% m/m based on *p*-cymene substrate). Both the precursors and their corresponding activated catalysts were tested as the actual catalyst for *p*-cymene liquid phase oxidations. The initiator containing 58% content of TCHP was obtained by concentrating the oxidized cymene oil under vacuum distillation by removing some of the unreacted *p*-cymene starting material. The desired reaction temperature was controlled at 100 °C by circulating the hot oil through the reactor jacket. The reactor temperature was continuously monitored during the experimental runs with a thermometer. For reaction temperature at 140 °C it was possible to do the oxidation reaction safely with pure O_2 due to the type of the reactor system used which was operated at ambient pressure under reflux conditions. This prevented any possible pressure build-up to occur that might cause a reaction explosion. The results at 140 °C showed slight deviations from the model's predicted outcomes. This was due to the difficulty posed by the reactor system used to be able to handle the high exothermic heat release at 140 °C. It is possible that some of the reactants vapour might have escaped during the reaction at the elevated temperatures. A reflux condenser attached to the reactor ensured the complete condensation and recycling of the evaporated compounds. The reaction mixture was stirred at a range of 250–2000 rpm stirrer speed. O_2 gas was introduced through a gas inlet tube at the top of the reactor at a flow rate of 40 mL min^{-1} after the reaction has been allowed for about 10 min to stabilize at the desired reaction temperature. The oxidation products samples containing the hydroperoxide were collected at regular intervals and treated with triphenylphosphine (0.02 g, 0.076 mmol) in methanol solvent (5 mL) for GC-FID analysis using a Supelco SPB-20 column (30 m × 0.25 mm i.d × 0.25 μm).

3. Results and discussion

3.1. Characterization of catalyst

Fig. 1 shows powder XRD analysis of the three precursors prepared by different methods. The prepared $VOHPO_4·0.5H_2O$ precursors (labeled P1, P2, P3) were calcined under N_2 to give the activated vanadyl pyrophosphate catalysts, $(VO)_2P_2O_7$ (labeled C1, C2, C3) in Fig. 2. XRD pattern of the P3 precursor is characterized by only one relatively strong peak at around 30.4° 2θ while precursor P1 and P2 showed a number of peaks in a range of 15.5–49.5° 2θ. The only single intense peak observed in P3 (2 2 0) making it different to P1 and P2 is the result of the preparation method and more specifically the alcohol type used (primary alcohol) to reduce the $VOPO_4·2H_2O$ to the catalyst precursor [14,24]. The XRD of the three activated precursors (C1, C2, C3) showed that the C1 and C3 catalysts had characteristic peaks similar to $(VO)_2P_2O_7$ phase while C2 displayed mainly an amorphous type phase with small visible peaks resembling the $(VO)_2P_2O_7$ phase (Fig. 2). Table 1 shows the BET surface areas and particle size distribution of the precursors and their corresponding activated catalysts. The P3 precursor prepared by the reduction of $VOPO_4·2H_2O$ with isobutanol resulted in a material with the smallest particle size, 16.7 μm and the largest surface area of 28.3 m^2 g^{-1} when compared to the other precursors. Its activated catalyst, C3 also showed the smallest particle size, 3.6 μm and the largest surface area of 38.5 m^2 g^{-1} when compared to the other activated catalysts. These results agree closely with the BET surface areas reported by Hutchings and co-workers [14].

3.2. Oxidation using different VPO catalysts

The different precursors and their calcined catalysts were tested in liquid phase oxidation of *p*-cymene. Table 1 and Fig. 3 summarize the oxidation results of the different catalysts studied. It is apparent from the results presented in Table 1 that some of the catalysts material showed improved selectivity towards TCHP when compared to oxidation carried out in the absence of a catalyst. Surprisingly, also the catalyst precursors showed a substantial catalytic activity in the *p*-cymene oxidation reaction. However, their

Table 1
Comparison of VPO catalysts catalytic performance in *p*-cymene oxidation.

Catalyst name	BET SA (m^2 g^{-1})	Particle size (μm)	TCHP (mol%)[a,b]	
			Selectivity	Yield
P1	2.1	34.4	61.7	9.2
P2	6.5	32.1	69.4	10.4
P3	28.3	16.7	84.6	12.7
C1	3.2	6.5	65.0	9.7
C2	14.5	4.6	72.7	10.9
C3	38.5	3.6	89.8	13.5

[a] Comparison of catalysts are based on 15% conversion.
[b] TCHP, Tertiary cymene hydroperoxide.
P1, P2 and P3 = $VOHPO_4·0.5H_2O$ precursors prepared by different methods.
C1, C2 and C3 = activated $(VO)_2P_2O_7$ catalysts prepared by different methods.
Reaction conditions: 35 g *p*-cymene, 2 g CHP initiator, 0.0175 g catalyst for catalyzed reactions, 40 mL min^{-1} flow rate, 2000 rpm stirring rate, 120 °C.

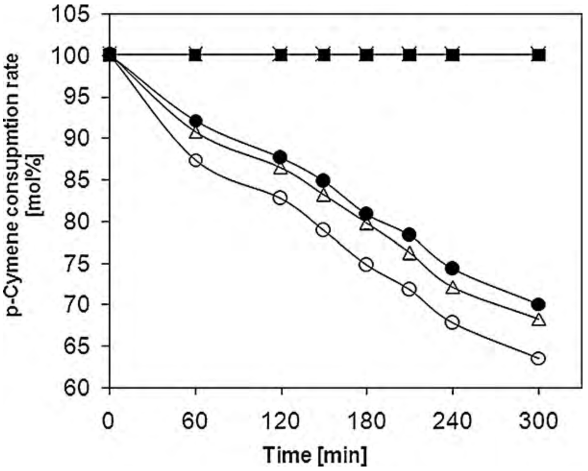

Fig. 3. Comparison of non-catalyzed and catalyzed with different catalysts *p*-cymene consumption rates. (■) non-catalyzed reaction; (□) C1 catalyst; (△) C2 catalyst; (○) C3 catalyst. (Other conditions: 35 g *p*-cymene, 2 g CHP initiator, 0.0175 g catalyst for catalyzed reactions, 40 mL min^{-1} flow rate, 2000 rpm, 120 °C).

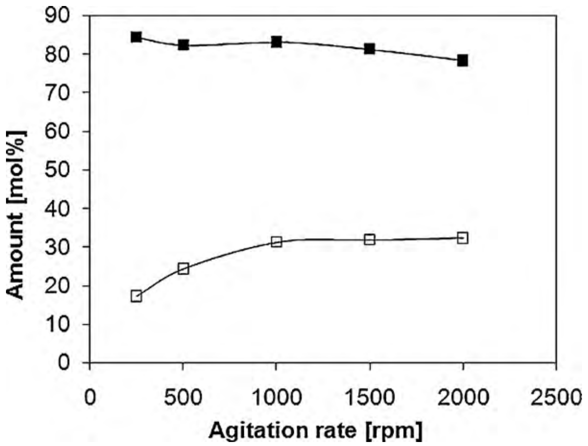

Fig. 4. Effect of the stirrer speed on conversion rates and TCHP selectivity. (□) conversion and (■) TCHP selectivity. (Other conditions: 35 g *p*-cymene, 0.05% C3 catalyst, 40 mL min^{-1} O_2 flow rate, and reaction time for each stirred speed point studied was fixed at 3 h).

respective TCHP selectivity was somewhat low when compared to their corresponding activated catalysts. The observed TCHP selectivity for catalyst precursors (P1, P2 and P3) and their activated catalysts (C1, C2 and C3) were closely related to their respective particle sizes and BET surface areas where an increase in the surface area seemed to give an increase towards TCHP selectivity (Table 1). Other factors such as vanadium oxidation state and the preferential exposure of the (2 0 0) plane of vanadyl pyrophosphate, $(VO)_2P_2O_7$ has been shown to play important role in the catalytic properties of the activated VPO catalyst [14]. However, in the present studies such catalyst microstructure properties effects on the TCHP selectivity were not studied in detail. The C3 catalyst gave a better TCHP selectivity when compared to the other catalysts under the same reaction conditions. There was, however, very little difference in the activities of the catalysts when comparing their respective rate of *p*-cymene consumption (Fig. 3).

Based on the results obtained for the use of both the precursors and their activated catalysts as the actual catalysts for the *p*-cymene oxidation, it seemed as if the vanadyl pyrophosphate phase ($(VO)_2P_2O_7$) known to be the active phase for gas phase oxidations is not necessarily required as the solely active phase for the liquid phase oxidation of *p*-cymene [7,8]. The actual surface area exposed to the bulk liquid appears to be of much greater importance than the types of catalyst phase following the trend of TCHP selectivity in relation to the catalyst's surface areas (Table 1). Hutchings and co-workers [14] showed that high catalytic performance of VPO catalyst is obtained from the $(VO)_2P_2O_7$ catalyst phase prepared from the method using the reduction of the intermediate $VOPO_4{\cdot}2H_2O$ phase to $VOHPO_4{\cdot}0.5H_2O$ precursors.

3.3. *Effect of stirrer speed on oxidation rates*

In order to investigate whether the liquid phase oxidation reaction, as performed in the well-stirred batch reactor showed any external mass transfer limitations, the effect of the stirring rate on *p*-cymene oxidation rates was investigated by using the C3 $(VO)_2P_2O_7$ catalyst and measuring the conversion rate of *p*-cymene during a fixed reaction period and other reaction conditions. The stirrer speed range chosen was between 250 and 2000 rpm to establish the speed at which the external mass transfer effect, if present, can be considered negligible. Fig. 4 illustrates the results of the effect of stirrer speed on the *p*-cymene conversion and oxidation rates. The observed trend clearly showed that below the stirrer speeds of approximately 1000 rpm, the reaction rate varied significantly with varying stirrer speeds. In this region, the reaction rate is clearly mass transfer limited, probably because of a diminished gas/liquid interfacial area as the slow stirrer speeds cannot effectively break up the gas bubbles into sufficiently smaller bubbles, nor disperse such bubbles effectively throughout the reaction mixture, thus enhancing the triphasic reactants contact. At stirrer speeds above approximately 1000 rpm, the reaction rate becomes virtually independent of stirrer speed; hence, in this region the reaction rate can presumably be kinetically controlled. The effect of stirrer speed on TCHP selectivity did show slight significant differences.

3.4. *Effect of catalyst on oxidation initiation rates*

The main role of the catalyst in liquid phase oxidations is to speed up the rates of reaction initiation by participating in the typical hydroperoxide decomposition either by deliberately adding an initiator, or formed as reaction product, thus forming free radicals [1,9]. In order to determine whether $(VO)_2P_2O_7$ catalyst does play a role in initiating the reaction or whether initiation was controlled only by the amount of added CHP oil as initiator, the *p*-cymene oxidation was firstly performed in the absence of catalyst and CHP initiator oil. The same oxidation reaction was repeated but in the presence of 0.05, 0.1, and 0.3% *m*/*m* C3 catalyst (based on used *p*-cymene). The *p*-cymene was firstly treated with aqueous 27% NaOH to remove any present residual hydroperoxides or peroxides. As can be seen in Fig. 5a the results showed that no product was formed during the initial 4–5 h reaction period in the absence of both catalyst and CHP initiator oil. When 0.05% of C3 catalyst was added in the absence of initiator, the reaction initiated after 180 min. When the catalyst concentration was doubled to 0.1%, the reaction initiated after 120 min to give *p*-cymene conversion of up about 18% after 5 h. With further increasing of catalyst concentration from 0.1 to 0.3% there was a significant improvement of the oxidation initiation rates with induction period of about 60 min and 23% conversion after 5 h. The impact of using high catalyst concentration is illustrated in Fig. 5b by the drop of TCHP selectivity with increasing catalyst concentration. This phenomenon can be explained by the possibility of the high rate of TCHP decomposition into by-products probably catalyzed by the high catalyst concentration. It is interesting to note that even in the absence of the added initiator the VPO catalyst displayed better initiation rates to activate the C–H bond to form the free radicals. In this case, the metal catalyst acts as both the initiator substrate and catalyst role. The observed initiation rates in the presence of the catalyst in differ-

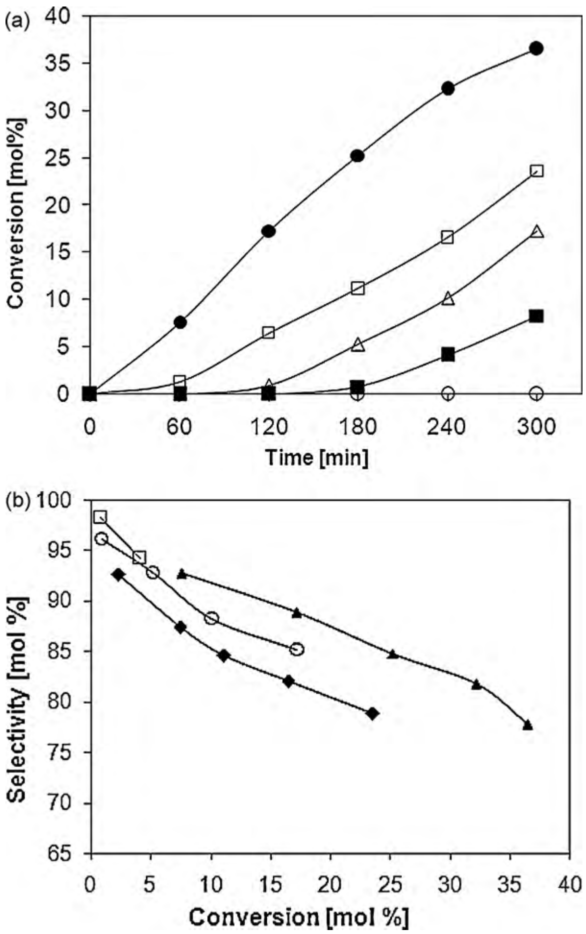

Fig. 5. Effect of the catalyst on *p*-cymene oxidation reaction initiation rates. (○) non-catalyzed with added initiator; (■) catalyzed with 0.05% catalyst and no initiator; (△) catalyzed with 0.1% catalyst and no initiator; (□) catalyzed with 0.3% catalyst and no initiator; (●) catalyzed with 0.05% catalyst and 2 g initiator added. Other conditions: 35 g *p*-cymene, 40 mL min^{-1} O_2 flow rate, 2000 rpm, 120 °C).

ent concentration (Fig. 5a) are much better when compared to for non-catalyzed reaction that takes up to 5–6 h. The reaction done in the presence of small amount of the cymene oil added as initiator (2 g) in the presence of 0.05% also showed better initiation rates of 30 min when compared to the reaction done only in the presence of 0.05% catalyst for 120 min. In the presence of the catalyst with added initiator (ROOH), the reaction initiation to form the free radicals has been shown to occur through the direct contact of the hydrocarbon with the catalyst itself [1]. The direct contact of the catalyst and hydrocarbon route to initiate the reaction rates in the present study showed to be slower than when the catalyst initiates the reaction with the decomposition of the added initiator substrate. The improved rise in the reaction rate in the catalyzed reaction with added initiator also indicated the active participation of catalyst in reaction initiation by speeding up the rate of cymene hydroperoxide initiator decomposition to form the free radicals, which in turn activate the *p*-cymene C–H bond energies to form further free radicals (Fig. 5a). This process continues as a repeated oxidation cycle until the chain reaction is terminated to form stable compounds.

The observed results indicated that the catalyst actively participates in the initiation of the *p*-cymene oxidation reaction since the addition of catalyst reduced the normal reaction induction periods of about 4–5 h to about 30–60 min. The initiation and oxidation rates in the presence of only catalyst showed that the build-up of hydroperoxide formation followed a typical autocatalytic behavior (Fig. 4). There was a typical slow increase in the rate of oxidation, which was followed by a rapid rise in reaction rate. This behavior can be explained in terms of the build-up of chain propagating species (mainly hydroperoxides) during the initial slow phase, followed by their participation in chain branching reactions (rapid rise in reaction rate) [1,26]. Since the build-up of the chain was more rapid in the presence of catalyst, and also since the same build-up was observed when more catalyst was used or initiator substrate was added, the direct participation of the catalyst in the actual initiation was clearly enunciated. Usually, once the critical concentration of chain branching species was reached, the observed rapid increase in reaction rate was better explained in terms of chain branching than in terms of the actual catalyst activity [1]. Leaching of vanadium metal in liquid phase oxidation of *p*-cymene process was shown previously to be negligible and the catalyst can be reused without significant loss of activity indicating that the catalytic reactions proceed as heterogeneous [28].

3.5. *Effect of the CHP initiator purity on oxidation rates*

Two reactions were done in order to establish whether and how the removal of the PCHP from the oxidized cymene hydroperoxide oil would affect the *p*-cymene oxidation rates and TCHP selectivity. First, the oxidation reaction was done with the unpurified CHP initiator oil (i.e. initiator oil containing both PCHP and TCHP) in the presence of 0.05% of C3 catalyst. The same *p*-cymene oxidation reaction was repeated but using purified CHP initiator (i.e. CHP initiator oil with PCHP removed) instead of unpurified. The purified CHP initiator was prepared by extracting the oxidized CHP oil with aqueous 27% NaOH to remove the PCHP. The GC analysis showed the complete removal of the PCHP and recovery of 98% of the TCHP. The results for comparison of purified and unpurified CHP initiators conversion rates are shown in Fig. 6a. As can be seen in Fig. 6 the use of the unpurified CHP initiator oil showed a slight advantage and consequently a somewhat better conversion rate after a reaction period of 6 h when compared to the purified CHP initiator oil. However, when the TCHP selectivity was compared for the two different CHP initiators as illustrated in Fig. 6b it was clear that the improved oxidation rates for the unpurified CHP initiator comes at the expense of TCHP selectivity. The improved TCHP selectivity was especially noticeable at conversion levels below 25% for purified CHP initiator when compared to unpurified initiator. At substrate conversions above 25%, the advantage of using purified CHP oil as initiator diminished. This was probably due to the slow increase of PCHP during the initial part of the reaction and the formation of other temperature induced-decomposition by-products of the *p*-cymene oxidation process such as *p*-methylacetophenone and *p*-isopropylbenzaldehyde.

3.6. *Effect of catalyst on hydroperoxide stability*

To determine the effect of VPO catalyst on hydroperoxide decomposition rate, two experiments were done in which the cymene hydroperoxide (CHP) oil containing TCHP was firstly decomposed under O_2 in the absence of the catalyst and then with 0.05% catalyst added. The mixture of the CHP was obtained through concentration of the previously oxidized *p*-cymene oil by distilling off some of the unreacted *p*-cymene. As can be seen in Fig. 7 for the CHP decomposition under O_2 in the absence of the catalyst, there was a gradual decrease of TCHP amount of 50.83% to about 3.9% after 120 min, while the TCHP decomposition in the presence of C3 catalyst showed rapid decomposition rate from about 50.83% TCHP to about 4% within 50 min. The decomposition rate of the TCHP in the presence of 0.05% C3 catalyst displayed the rate with a factor of 2.5 times faster than in the presence of O_2 only. The major decomposition product formed in both cases, decomposition under O_2

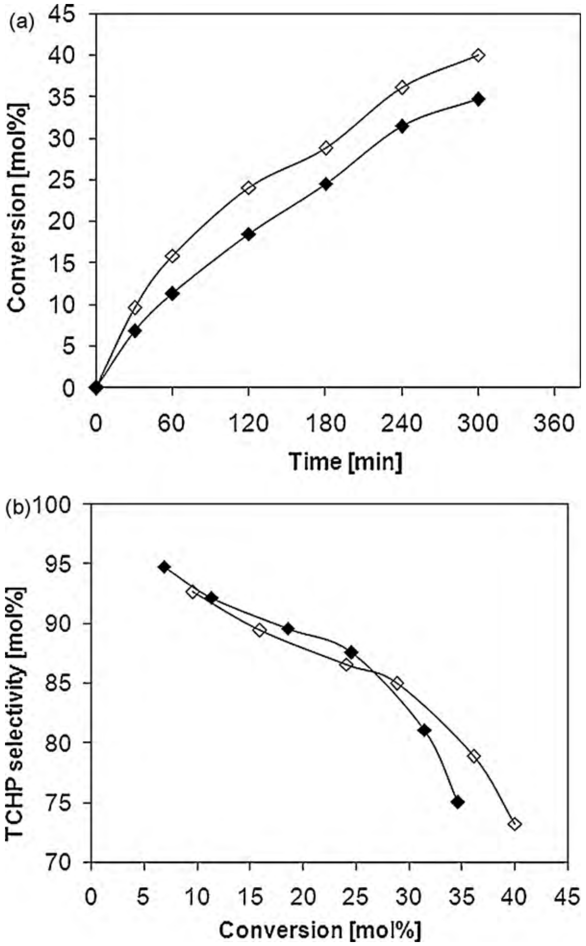

Fig. 6. Effect of the initiator purity on (a) *p*-cymene oxidation rates and (b) TCHP selectivity. (♦) unpurified CHP initiator; (■) purified CHP initiator. (Reaction conditions: 35 g *p*-cymene, 0.05% C3 catalyst, 40 mL min^{-1} O_2 flow rate, 2000 rpm, 120 °C).

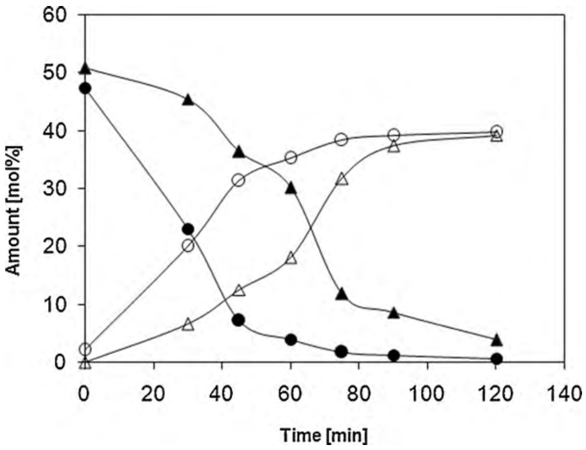

Fig. 7. TCHP decomposition rate under only O_2 conditions and O_2 in the presence of 0.05% catalyst. (▲) TCHP-no catalyst; (●) TCHP–with catalyst; (△) MMVB–no catalyst; (○) MMVB–with catalyst. (Other conditions: oxidized cymene hydroperoxide oil (35 g), 40 mL min^{-1} O_2 flow rate, 2000 rpm stirring rate, 120 °C).

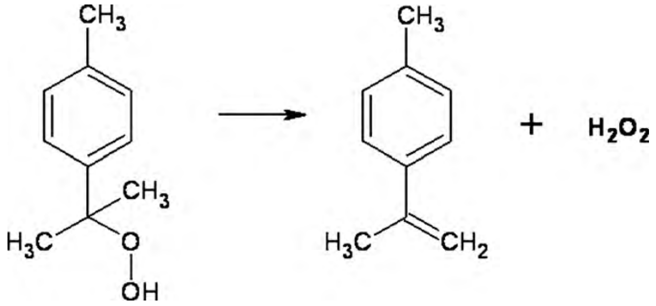

Scheme 2. Hydrolysis decomposition of tertiary cymene hydroperoxide to 1-methyl-4-(1-methylvinyl) benzene (MMVB)

conditions in the absence and presence of catalyst was identified as 1-methyl-4-(1-methylvinyl) benzene (MMVB). The decomposition rate of TCHP in the experiment done with oxidized cymene oil (concentrated to TCHP content of about 50.83%) and 0.05% catalyst under O_2 conditions was faster when compared to the normal oxidation process (i.e. oxidation of *p*-cymene in the presence of CHP initiator and catalyst). Under the normal oxidation process, only less than 1% amount of MMVB formation was observed at conversions above 35%. This shows the instability and sensitivity of hydroperoxide products in liquid phase oxidations to temperature and thus, selectivity to the desired products especially at high substrate conversions. Mostly, conversions are restricted to low in liquid phase oxidation processes as to preserve the acceptable desired product selectivity [1,26]. As a result, the improved selectivity to TCHP as seen in Fig. 6 and Table 1 may be probably explained in terms of the inability or slow rate of the VPO catalyst to catalyze the hydroperoxide decomposition during the normal *p*-cymene oxidation process. The formation of MMVB can be explained by the hydrolysis decomposition of the tertiary cymene hydroperoxide, which undergoes rearrange to form hydrogen peroxide and MMVB as illustrated by Scheme 2 from TCHP. This reaction is similar to the reported decomposition reaction process of tertiary butyl hydroperoxide in the presence of solid acidic catalyst to produce hydrogen peroxide [27].

3.7. Effect of temperature on oxidation rates

Four different reaction temperatures (80, 100, 120 and 140 °C) were chosen to study their effect on *p*-cymene oxidation rates using C3 catalyst and both the conversion of *p*-cymene as well as the TCHP selectivity were monitored. Fig. 8 illustrates the results for the effect of temperature on oxidation rates and selectivity. The results showed that higher reaction temperatures improved significantly the *p*-cymene oxidation and conversion rates. At 140 °C, a conversion of 35% was achieved within the 3 h reaction period, while at a reaction temperature of 80 °C, a conversion of only 15% was observed after 3 h. However, at high reaction temperatures, selectivity to TCHP decreases significantly (Fig. 8b). This observation can be explained in terms of the higher rate of TCHP and PCHP decomposition (probably catalyzed) at these higher reaction temperatures. At substrate conversion below 10% reaction temperatures of 80, 100 and 120 °C showed closely related TCHP selectivity while above ca.10% conversion a clear difference in their TCHP selectivity was observed (Fig. 8b). To achieve acceptable TCHP selectivity a reasonable level of substrate conversion will need to be a compromise between the desired reaction time, rate of oxidation and product yield.

3.8. Kinetic considerations of *p*-cymene autoxidation

The autoxidation of hydrocarbons proceeds via a radical chain mechanism that involves a large number of radical and molecular species [1,4,6,26,29–35]. The complexity of this reacting species makes difficult to accurately evaluate the individual values of the kinetic constants by direct fitting of model results against experiment data, because of the inability of measuring the concentration of the radical species. In order to overcome these complications,

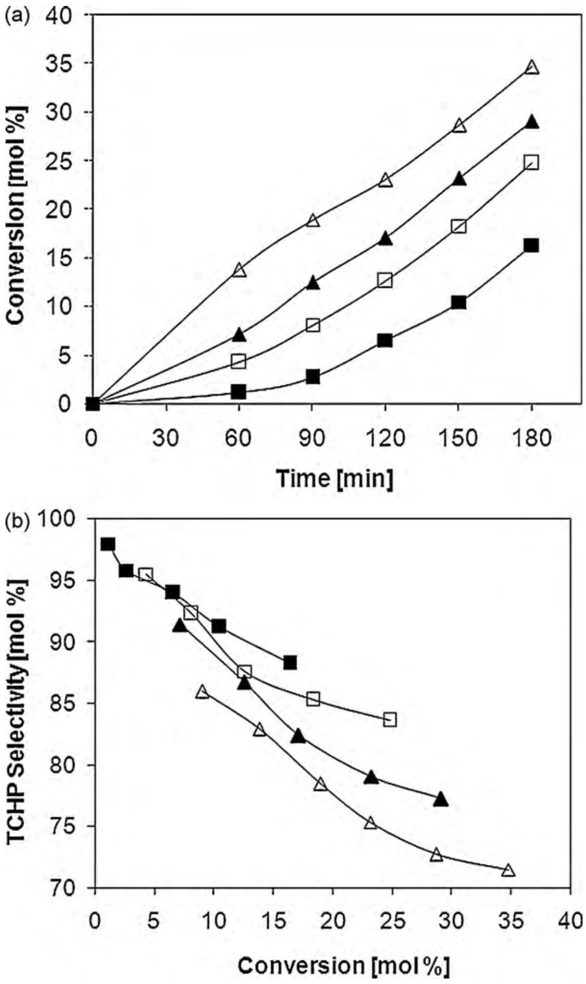

Fig. 8. The effect of reaction temperature on (a) cymene conversion rats and (b) TCHP selectivity. Symbols: (■) 80 °C, (□) 100 °C, (▲) 120 °C and (△) 140 °C. (Other conditions: 35 g *p*-cymene, 0.05% C3 catalyst, 40 mL min^{-1} O_2 flow rate, 2000 rpm).

the common approach is to put together the detailed mechanism into a set of typical reactions that involve only the molecular species, whose concentrations can be practically measured as a function of time [29–34]. By accounting these measurable concentrations of the molecular species, the kinetic model can be proposed that will describe the radical chain reactions for the consumption of substrate and formation of products. To be able to establish the kinetic model to evaluate the obtained experimental *p*-cymene oxidation results the well-studied cumene kinetic model was used in the present study. Both compounds contain the isopropyl group attached to the benzene; however, *p*-cymene has an additional methyl group at para position. The kinetic model derivation approach used by Hattori et al. [4] and Bhattacharya [5] were used to define the kinetic model to predict the experimental outcome of the *p*-cymene oxidation results. This was done by proposing two rate equations for cumene consumption (Eq. (1)) and cumene hydroperoxide formation (CHP) (Eq. (2)) following several simplified assumptions [4,5] given as:

$$-\frac{\mathrm{d[RH]}}{\mathrm{dt}} = K[\mathrm{RH}]\sqrt{[\mathrm{ROOH}]} + 2k_1[\mathrm{ROOH}] \tag{1}$$

$$\frac{\mathrm{d[CHP]}}{\mathrm{dt}} = K[\mathrm{RH}]\sqrt{[\mathrm{ROOH}]} - k_1[\mathrm{ROOH}] \tag{2}$$

Table 2
Estimated and calculated values of *K* and k_1.

Temperature (°C)	*K*	k_1
80	0.035	0.50
100	0.054	0.75
120	0.071	1.02
140	0.095	1.50

In the above equations, *K* is defined as the “effective” or overall rate constant, given by Eq. (3):

$$K = \frac{p_{O_2} k_3/\mathrm{H[RH]_{av}}}{1 + p_{O_2} k_3/k_4\mathrm{H[RH]_{av}}}\sqrt{\frac{k_1}{k_{13}}} \tag{3}$$

From the preceding discussions on the kinetic model of cumene autoxidation, it should be obvious that the kinetic scheme for *p*-cymene will be considerably more complex in view of the possibility of oxidation happening on the methyl group of *p*-cymene. In effect, each of the elementary reaction steps written for the oxidation of the isopropyl group can also be written for the methyl group. This would result in an even more complex set of kinetic parameters to be solved simultaneously. The same simplified model for cumene autoxidation reported by Hattori et al. [4], was used to develop a simplified model to describe the oxidation of *p*-cymene as well. In developing this model, we made a first assumption that the rate of initiation, by thermal decomposition of the tertiary cymene hydroperoxide, will not be significantly different from the rate of cumene hydroperoxide decomposition. Thus, as a first approximation the value of the rate constant k_1 (Eqs. (1) and (2)) was assumed to be the same for both cumene and *p*-cymene oxidation systems. The second assumption that was made was that the contribution of the methyl group in *p*-cymene to: (a) Additional elementary reaction steps leading to the consumption of *p*-cymene; and (b) The rate of oxidation of the isopropyl group, can be lumped together in the overall rate constant *K* (Eqs. (1) and (2)). Having made these simplifying assumptions, and using the Arrhenius parameters for the rate constant k_1 as reported by Bhattacharya [5], values for the overall rate constant *K* for *p*-cymene oxidation was estimated by regression and minimizing the sum of error squares during these regressions. A fairly good comparison of predicted and experimental results of *p*-cymene consumption and cymene hydroperoxide formation as a function of reaction time at different temperatures (80, 100, 120 and 140 °C) in a well-stirred batch reactor were obtained (Fig. 9). The results at 140 °C showed slightly significant deviation from the model predicted outcomes. This is due to the difficulty posed by the reactor system used, which was operated at atmospheric pressure to be able to handle the high exothermic heat release accompanied by some reaction mixture vapour at 140 °C. Table 2 lists the values of *K* estimated from the regressions, as well as the values of k_1. Fig. 9 shows the Arrhenius plots for *K* and k_1, respectively.

Figs. 9 and 10 showed that the simplified kinetic model for cumene autoxidation as proposed by Hattori et al. [4] could also be used to describe the autoxidation of *p*-cymene, despite the significantly more complex reaction scheme for *p*-cymene. The estimated value for the “overall” rate constant (*K*) for *p*-cymene ($0.071\,\mathrm{s}^{-1}$) compares very favourably with the values reported for cumene by Hattori et al. [4] ($0.093\,\mathrm{s}^{-1}$) and Bhattacharya [5] ($0.083\,\mathrm{s}^{-1}$). The lower value for K for *p*-cymene is in agreement with the observed lower oxidation rate of *p*-cymene as compared to cumene. The values estimated for *K* for *p*-cymene autoxidation and shows typical Arrhenius behavior (Fig. 10a) with: $E_a = 19.88\,\mathrm{kJ\,mol^{-1}}$; and $A = 31.19\,\mathrm{min}^{-1}$.

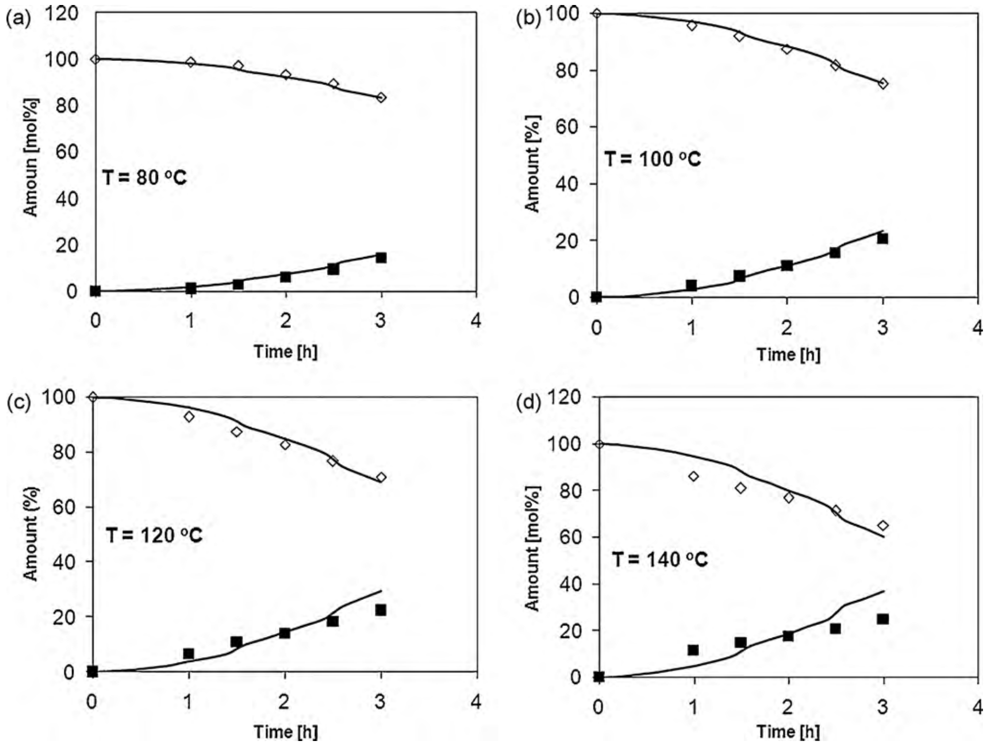

Fig. 9. Comparison of the *p*-cymene kinetic model predicted and experimental observed results at 80, 100, 120 and 140 °C. Symbols: (◇) RH = *p*-cymene; (■) ROOH = cymene hydroperoxide; and line represent both predicted RH and ROOH model outcomes.

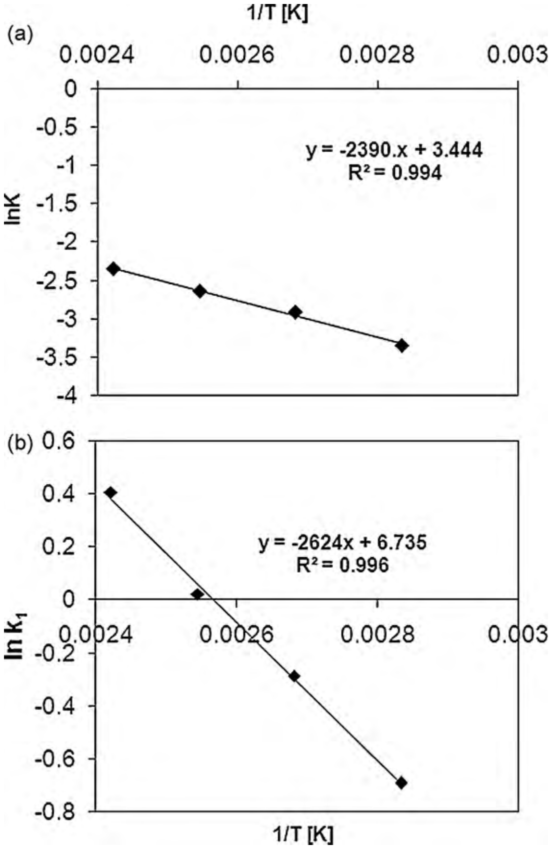

Fig. 10. Plot of (a) ln *K* vs. 1/*T* and (b) ln k_1 vs 1/*T*.

4. Conclusions

The liquid phase oxidation of *p*-cymene to TCHP using VPO based catalyst was demonstrated in a well-stirred batch reactor. The process gave a better conversion and productivity rate when compared to the commercial industrial-scale process. Conversions of about 30% within 3 h were obtained at 80% TCHP selectivity. While the exact role of the catalyst remains obscure, the results clearly showed that the vanadyl pyrophosphate phase, $(VO)_2P_2O_7$ known to be the active phase for selective gas phase oxidations, was not necessarily required as the solely active phase for the liquid phase oxidation of *p*-cymene. The results also showed that there appears to be direct participation of the catalyst in the initiation process. On the other hand, the catalyst showed slow yet significant influence on the decomposition rate of the hydroperoxide studied under O_2 conditions while under the normal oxidation reaction the catalyst showed insignificant or slow influence on the decomposition rate of the formed hydroperoxide during reaction at substrate conversions below 30%. This observation could possibly be one of the explanations of the better obtained TCHP selectivity when VPO was used as catalyst for *p*-cymene liquid phase oxidation. The results of the model gave reasonably good predicted observations for *p*-cymene consumption and *p*-cymene hydroperoxide formation rate related to the experimentally observed outcomes.

Acknowledgement

The authors thank Sasol, DST/NRF and Technology Institute Association (TIA) for financial support towards this research work.

References

[1] R.A. Sheldon, J.K. Kochi, Metal-Catalyzed Oxidation of Organic Compounds, Academic Press, New York, 1981.

[2] H. Fiege, Cresols and xylenols Ullmann's Encyclopedia of Industrial Chemistry, vol. A8, VCH Verlagsgesellschaft, 1991, p.25.

[3] K.E. Clonts, R.A. McKetta, Kirk-Othmer (3rd Ed.), Encyclopedia of Chemical Technology: Cresols and Cresylic Acids, Vol.3, Interscience, New York, 1978, pp. 212.

[4] K. Hattori, Y. Tanaka, H. Suzuki, T. Ikawa, H. Kubota, kinetics of liquid phase oxidation of cumene in bubble column, J. Chem. Eng. Japan 3 (1970) 72–78.

[5] A. Bhattacharya, Kinetic modeling of liquid phase autoxidation of cumene, Chem. Eng. J. 137 (2008) 308–319.

[6] G.S. Serif, C.F. Hunt, A.N. Bourns, Liquid phase oxidation of *p*-cymene: nature of intermediate hydroperoxide and relative activity of the alkyl groups, Can. J. Chem. 31 (1953) 1229–1238.

[7] K. Aït-Lachgar, M. Abon, J.C. Volta, Selective oxidation of *n*-butane to maleic anhydride on vanadyl pyrophosphate, J. Catal. 171 (1997) 383–390.

[8] S.H. Sookraj, D. Engelbrecht, Selective oxidation of light hydrocarbons over promoted vanadyl pyrophosphate, Catal. Today 49 (1999) 161–169.

[9] G. Landi, L. Lisi, G. Russo, Oxidation of propane and propylene to acrylic acid over vanadyl pyrophosphate, J. Mol. Catal. A: Chem. 23 (2005) 172–179.

[10] U. Bentrup, A. Brückner, A. Martin, B. Lücke, Selective oxidation of *p*-substituted toluenes to the corresponding benzaldehydes over $(VO)_2P_2O_7$: an in situ FTIR and EPR study, J. Mol. Catal. A: Chem. 162 (2000) 391–399.

[11] Y.H. Taufig-Yap, C.S. Saw, Effect of different calcinations environments on the vanadium phosphate catalysts for selective oxidation of propane and n-butane, Catal. Today 131 (2008) 285–291.

[12] G. Centi, F. Trifiró, Mechanistic aspects of maleic anhydride synthesis from C_4 hydrocarbons over phosphorus vanadium oxide, Chem. Rev. 88 (1988) 55–80.

[13] E. Bordes, Reactivity and crystal chemistry of V–P–O phases related to C_4-hydrocarbon catalytic oxidation, Catal. Today 3 (1988) 163–174.

[14] C.J. Kiely, A. Burrows, S. Sajip, G.J. Hutchings, M.T. Sananes, A. Tuel, J.C. Volta, Characterization of variations in vanadium phosphate catalyst microstructure with preparation route, J. Catal. 162 (1996) 31–47.

[15] J. Lui, F. Wang, Z. Gu, X. Xu, Vanadium phosphorous oxide catalyst modified by silver doping for mild oxidation of styrene to benzaldehyde, Chem. Eng. J. 151 (2009) 319–323.

[16] U.R. Pillai, E. Sahle-Demessie, Vanadium phosphorus oxide as an efficient catalyst for hydrocarbon oxidations using hydrogen peroxide, New J. Chem. 27 (2003) 525–528.

[17] M. Di Serio, M. Cozzolino, R. Tesser, P. Patrono, F. Pinzari, B. Bonelli, E. Santacesaria, Vanadyl phosphate catalysts in biodiesel production, Appl. Catal. A: Gen. 320 (2007) 1–7.

[18] A. Datta, M. Agarwal, S. Dasgupta, R.Y. Kelkar, A.R. Saple, Characterization and catalytic activity of novel palladium-incorporated vanadium phosphates, J. Mol. Catal. A: Chem. 181 (2002) 119–127.

[19] F. Wang, L.C. Dubois, W. Ueda, Catalytic dehydration of glycerol over vanadium phosphate oxides in the presence of molecular oxygen, J. Catal. 268 (2009) 260–267.

[20] P. Borah, A. Datta, Exfoliated VOPO4·2H2O dispersed on alumina as a novel catalyst for the selective oxidation of cyclohexane, Appl. Catal. A: Gen. 376 (2010) 19–24.

[21] A. Datta, S. Sakthikel, S.J. Kumar, US Patent 7586014132, 2009, Assign to Council of Scientific and Industrial Research, New Delhi.

[22] U.R. Pillai, E. Sahle-Demessie, R.S. Varma, Alternative routes for catalyst preparation: use of ultrasound and microwave irradiation for the preparation of vanadium phosphorus oxide catalyst and their activity for hydrocarbon oxidation, Appl. Catal. A: Gen. 252 (2003) 1–8.

[23] K. You, B. Wu, L. Mao, D. Yin, P. Liu, H. Lu, A novel route to one-step formation of ε-caprolactam from cyclohexane and nitrosyl sulfuric acid catalyzed by VPO composites, Catal. Lett. 118 (2007) 129–133.

[24] G.J. Hutchings, M.T. Sananes, S. Sajip, C.J. Kiely, A. Burrows, I.J. Ellison, J.C. Volta, Improved method for preparation of vanadium phosphate catalysts, Catal. Today 33 (1997) 161–171.

[25] Powder diffraction files PDF-2, International Centre for Diffraction Data, Pennsylvania, USA, Release 2004.

[26] A.K. Suresh, M.M. Sharma, T. Sridhar, Engineering aspects of industrial liquid-phase oxidation of hydrocarbons, Ind. Eng. Chem. Res. 39 (2000) 3958–3997.

[27] R. Rosenthal, J. Kieras, Continuous process for production of hydrogen peroxide, US, 3891748, 1975.

[28] P.R. Makgwane, E.E. Ferg, B. Zeelie, Characterisation and long-term usage catalytic properties of $(VO)_2P_2O_7/\gamma\text{-}Al_2O_3$ stainless steel coated catalyst in *p*-cymene oxidation, Appl. Catal. A: Gen. 373 (2010) 132–139.

[29] T.G. Traylor, C.A. Russell, Mechanisms of autoxidation: terminating radicals in cumene autoxidation, J. Am. Chem. Soc. 87 (1965) 3698–3706.

[30] D.G. Hendry, Rate constants for oxidation of cumene, J. Am. Chem. Soc. 89 (1967) 5433.

[31] R. Pohorecki, J. Baldyga, W. Moniuk, W. Podgorskya, A. Zdrojkowski, P.T. Wierzchowski, Kinetic model of cyclohexane oxidation, Chem. Eng. Sci. 56 (2001) 1285–1291.

[32] S.M. Mahajani, M.M. Sharma, T. Shridhar, Uncatalysed oxidation of cyclohexene, Chem. Eng. Sci. 54 (1999) 3967–3976.

[33] I. Hermans, Mechanism of thermal toluene autoxidation, ChemPhysChem 8 (2007) 2678–2688;
I. Hermans, J. Peeters, P.A. Jacobs, Autoxidation of ethylbenzene: the mechanism elucidated, J. Org. Chem. 72 (2007) 3057–3064.

[34] I. Hermans, T. Nguyen, P.A. Jacobs, J. Peeters, Autoxidation of cyclohexane: conventional views challenged by theory and experiment, ChemPhysChem 6 (2005) 637–645.

[35] I. Hermans, P.A. Jacobs, J. Peeters, To the core of autocatalysis in cyclohexane autoxidation, Chem. Eur. J. 12 (2006) 4229–4240.